Electron mass scattering powers: Monte Carlo and analytical calculations

X. Allen Li[a] and D. W. O. Rogers[b]
Ionizing Radiation Standards, Institute for National Measurement Standards, National Research Council Canada, Ottawa K1A 0R6 Canada

(Received 13 December 1993; resubmitted 13 December 1994; accepted for publication 31 January 1995)

Values of electron mass scattering power, T/ρ, for various materials have been calculated by using the EGS4 Monte Carlo system and by integration of the Molière multiple-scattering distribution. The energy range covered is 0.5–100 MeV. Monte Carlo calculations test the concept of T/ρ "experimentally" and assess the contribution to electron mass scattering power from effects such as Moller scatter and energy-loss straggling. The Monte Carlo results agree within 2% with the analytical results calculated from Molière multiple-scattering theory at energies less than 20 MeV for high-Z materials and for energies less than 50 MeV for low-Z materials. At higher energies the Monte Carlo calculations include the effects of bremsstrahlung production which can significantly increase values of T/ρ. For low-Z materials and electron energies less than 60 MeV, the Monte Carlo calculated T/ρ values are generally 22% higher than those given by ICRU Report 35, while those for high-Z materials and energies less than 25 MeV are found to be consistent (within 1%) with ICRU Report 35. The effects of Moller scatter, which significantly affect T/ρ for low-Z materials, as well as bremsstrahlung effects, are included in the present Monte Carlo calculations. If the tabulated T/ρ data of ICRU Report 35 are modified to include the Moller scatter effect, then for energies less than 60 MeV they are generally 6% less than the present Monte Carlo data for low-Z materials as well as for copper. It is shown that T/ρ is a well-defined constant over an appropriate range of slab thickness except when bremsstrahlung effects are significant. It is found that T/ρ is proportional to E^{-n}, where n is in the range of 1.5–2.0 for the energies considered here. The Monte Carlo calculations are shown to agree well with various relevant experimental measurements. Accurate T/ρ data, which should include the effect of Moller scatter, are necessary in electron-beam treatment planning, especially for a small field size. The choice of the depth step in the implementation of pencil-beam codes should not violate the slab-thickness limits for T/ρ data.

I. INTRODUCTION

In radiation dosimetry and radiotherapy, it is often important to have accurate information about the penetration of electron beams in matter. Electrons passing through matter are influenced in two fundamentally different ways by their collisions with the atoms of the absorber. Their energy is decreased by inelastic collisions and their direction is changed by multiple scattering. The average energy loss of electrons is well represented by the mass stopping power, while the change in direction of the electrons is often characterized by the mass scattering power, (T/ρ), which is defined[1,2] as the increase in the mean square angle of scattering $(d\overline{\theta^2})$ per unit mass thickness traversed $(\rho\, ds)$, i.e.,

$$\frac{T}{\rho}=\frac{d\overline{\theta^2}}{\rho\, ds}\ [\mathrm{rad^2\,cm^2\,g^{-1}}]. \tag{1}$$

Strictly speaking, this definition holds only for a zero thickness slab $(ds\rightarrow 0)$ but in practice it is usually applied to slabs of finite thickness. In fact, the concept is only of practical interest because the equation holds for slabs of finite thickness.

Assuming small and independent deflections, Rossi[3] has derived two expressions for mass scattering power based on slightly different theories which are valid for intermediate energies. In the first method he used the classical Rutherford scattering cross section. Screening of the nucleus by the atomic electrons was taken into account by setting the cross section to zero below a screening angle, $\theta_{\min}$ (all angles are in radians), which is related to the size of the atom. The finite size of the nucleus was taken into account by setting the cross section to zero above a maximum angle $\theta_{\max}$, which is related to the size of the nucleus. These two angles were based on simple models and $\theta_{\max}$ was further limited to values ≤ 1 rad, which in practice means $\theta_{\max}$ is 1 except at high energies. The formulas developed this way were used to tabulate values of the mass scattering power in ICRU Report 21.[1]

In his second approach, Rossi used a screened Rutherford cross section which is finite at zero degrees and explicitly includes the same screening angle $\theta_{\min}$. This leads to

$$\frac{T}{\rho}=\pi\left(\frac{2r_eZ}{(\tau+1)\beta^2}\right)^2\frac{N_A}{M_A}\left(\ln\left(1+\left(\frac{\theta_{\max}}{\theta_{\min}}\right)^2\right)-1+\left(1+\left(\frac{\theta_{\max}}{\theta_{\min}}\right)^2\right)^{-1}\right)\ [\mathrm{rad^2\,cm^2\,g^{-1}}], \tag{2}$$

where $\theta_{\max}$ has the same meaning as above and r_e, Z, τ, β, N_A, and M_A are the electron classical radius, atomic number, ratio of kinetic energy of the electron to its rest energy, velocity of the electron relative to the velocity of light in vacuum, Avogadro's constant, and molar mass of the substance (g/mole), respectively. Since the derivation of this equation assumes independent deflections from each atom, values of T/ρ for compounds are calculated by adding the values for each element according to their fraction by weight. Note that Rossi left out the last term because it has a negligible effect but it was reinserted in ICRU Report 35[4]

 0094-2405/95/22(5)/531/11/$6.00

which uses this formula to tabulate values of T/ρ (we find that our programs do not always get the exact values tabulated in ICRU35 although we get exact agreement with other sources).

The selection of the screening angle, $\theta_{\min}$, is important since its value affects the value of T/ρ. Rossi and others use a simple model for $\theta_{\min}$, viz., $\theta_{\min}=\lambda/(2\pi r_a)$ where r_a is the atomic radius and λ is the wavelength of the electron. For Rossi this reduces to $\theta_{\min}=\alpha Z^{1/3}/\beta(\tau+1)$ where α is the fine structure constant, whereas ICRU Report 35 uses a 13% larger value which just reflects using the Thomas–Fermi value of the atomic radius. The value for $\theta_{\max}$ (taken as $\lambda/(2\pi r_n)$ where r_n is the nuclear radius) also affects the value of T/ρ but for the energies of interest here, its value is almost always 1 rad, which is somewhat arbitrarily selected.

If one assumes that the deflections of the particles in the slab are due to a large number of small and independent deflections, then the angular distributions of the electrons are Gaussian in shape. In practice, T/ρ values are used to give the width of this distribution, in particular in treatment planning algorithms based on Fermi–Eyges theory (e.g., Hogstrom *et al.*[5]). It is well known,[4] and we shall see below that this prediction of a Gaussian shape is not in good agreement with experimental measurements which have significant large-angle tails which are primarily due to one or a few large-angle scattering events.[6]

The values of electron mass scattering power tabulated in ICRU Reports 21 and 35 do not include the effects of electron–electron scattering (Moller scatter) although ICRU Report 35 mistakenly asserts that the values in ICRU Report 21 include it. The values of T/ρ given by ICRU Report 35 are of the order of 12% less than those given by ICRU Report 21 at low energies; the difference decreases to about 6% at 50 MeV.

More recently, McParland[7] has reported another calculation based on the scattering cross section derived by Mott which accounts for the electron spin. His approach does not explicitly use a small-angle approximation. Values of the electron mass scattering power calculated from his expression, which is only valid for low-Z materials ($Z<27$), are approximately 6% less than those in ICRU Report 35. Huizenga and Storchi[8] have also introduced an estimate of T/ρ based on the Gaussian term of the Molière multiple-scattering theory[9,10] which is discussed below. This estimate has the unfortunate feature of making T/ρ depend on the slab thickness. As will be seen below, retaining all terms in Molière theory leads to values for T/ρ which are independent of slab thickness.

The above review suggests that T/ρ is sensitive to the theory used in the calculation. The Molière multiple-scattering theory[9,10] is a widely accepted theory which has been shown to be in much better agreement with experiment than using a Gaussian model with the mass scattering power predicted by the above approaches.[11] The Molière theory predicts the entire angular distribution which can be directly tested. Using this theory we report detailed analytical and Monte Carlo calculations of the values of the mass scattering power for lead, graphite, copper, water, and air in the energy range of interest in radiation dosimetry. In addition to studying the relation of the mass scattering power to the electron energy by Monte Carlo and analytical methods, particular attention has been focused on the differences between the analytic Molière calculations and the Monte Carlo calculations which are based on the same multiple-scattering theory but also include other effects. The effects of various transport parameters in the Monte Carlo calculations are also studied in order to obtain accurate values of T/ρ.

A major objective of this article is to examine the range of validity of the concept of a mass scattering power which is defined for a zero thickness slab but which is used in practical situations for slabs of finite thickness. The Monte Carlo technique is used to test the layer-thickness dependence of T/ρ "experimentally," and to assess the size of the contribution to electron mass scattering power from Moller scatter and energy-loss straggling. To complete the article, the Hogstrom pencil-beam code[5] for electron-beam dose calculation has been employed to study briefly the impact of using more accurate T/ρ values on electron-beam treatment planning.

II. MOLIÈRE MULTIPLE-SCATTERING THEORY AND ANALYTICAL CALCULATION

Electron elastic collisions with the atomic nucleii can be treated by the Molière multiple-scattering theory.[9,10] Molière used the small-angle version of the screened Rutherford cross section and assessed the screening effects using the Fermi–Thomas atomic model. His theory gives the angular distribution as the series

$$f(\theta)\theta\, d\theta=\vartheta\, d\vartheta[2e^{-\vartheta^2}+B^{-1}f^{(1)}(\vartheta)+B^{-2}f^{(2)}(\vartheta)+\cdots], \tag{3}$$

$$f^{(n)}(\vartheta)=\frac{1}{n!}\int_0^\infty u\, du\, J_0(\vartheta u)e^{-u^2/4}\left(\frac{u^2}{4}\ln\frac{u^2}{4}\right)^n, \tag{4}$$

where $\vartheta=\theta/\chi_c B^{1/2}$ is the reduced angle, B is defined by $B-\ln B=\ln\Omega_0$, J_0 is the zero-order Bessel function, and χ_c is given below. Ω_0 can be interpreted as the number of atomic collisions that contribute to the scattering and is related to the step length. Molière considered his theory valid for $\Omega_0>20$. Recent work has shown that the Molière multiple-scattering theory as implemented in EGS4 is reasonably accurate compared to detailed Monte Carlo calculations which simulate individual elastic scattering, as long as the limit $\Omega_0>20$ is obeyed.[12]

Although originally derived as a small-angle theory, Molière multiple-scattering theory has been modified by Bethe to predict accurately large-angle scattering[13] and we include this correction by multiplying the right hand side of Eq. (3) by $\sqrt{\theta/\sin\theta}$. Molière theory applies to arbitrary step sizes within a given range. The minimum step size ($t_{\min}$) required to ensure sufficient scatter is given by[10,14]

$$t_{\min}=\Omega_0\beta^2/b_c\ \text{[cm]}, \tag{5}$$

with $\Omega_0=20$, while the maximum step size ($t_{\max}$) derived by Bethe[13] in his treatment of the Molière theory is

TABLE I. The low and high limits of the slab thickness, s_{min} and s_{max}, in g/cm^2, used in the present calculations. The value of s_{min} is selected to ensure at least 20 interactions occur so that multiple-scattering theory applies. The value of s_{max} ensures no more than a 2% energy-loss correction is required.

Kinetic energy (MeV)	Graphite		Lead		Water		Air		Copper	
	s_{min}	s_{max}	s_{min}	s_{max}	s_{min}	s_{max}	s_{min}	s_{max}	s_{min}	s_{max}
0.5	0.002 11	0.0113	0.002 80	0.0178	0.002 54	0.009 94	0.002 04	0.0112	0.001 76	0.0145
0.8	0.002 41	0.0158	0.003 19	0.0236	0.002 90	0.0139	0.002 32	0.0155	0.002 01	0.0199
1	0.002 51	0.0186	0.003 34	0.0269	0.003 03	0.0163	0.002 42	0.0181	0.002 09	0.0231
2	0.002 72	0.0310	0.003 61	0.0400	0.003 28	0.0271	0.002 62	0.0294	0.002 27	0.0368
3	0.002 78	0.0424	0.003 69	0.0499	0.003 34	0.0371	0.002 68	0.0394	0.002 32	0.0485
4	0.002 80	0.0532	0.003 72	0.0581	0.003 37	0.0466	0.002 70	0.0488	0.002 33	0.0582
5	0.002 81	0.0635	0.003 73	0.0649	0.003 39	0.0557	0.002 71	0.0577	0.002 34	0.0683
8	0.002 82	0.0927	0.003 75	0.0801	0.003 40	0.0814	0.002 73	0.0823	0.002 36	0.0921
10	0.002 83	0.111	0.003 76	0.0873	0.003 41	0.0975	0.002 73	0.0974	0.002 36	0.105
15	0.002 83	0.153	0.003 76	0.0996	0.003 41	0.134	0.002 73	0.132	0.002 36	0.131
20	0.002 83	0.190	0.003 76	0.107	0.003 41	0.167	0.002 73	0.162	0.002 36	0.149
30	0.002 83	0.255	0.003 77	0.116	0.003 42	0.222	0.002 73	0.213	0.002 36	0.175
40	0.002 83	0.308	0.003 77	0.120	0.003 42	0.269	0.002 74	0.256	0.002 36	0.191
50	0.002 83	0.354	0.003 77	0.123	0.003 42	0.307	0.002 74	0.293	0.002 37	0.203
60	0.002 83	0.392	0.003 77	0.124	0.003 42	0.340	0.002 74	0.324	0.002 37	0.211
80	0.002 84	0.455	0.003 77	0.126	0.003 42	0.393	0.002 74	0.376	0.002 37	0.223
100	0.002 84	0.503	0.003 77	0.127	0.003 42	0.434	0.002 74	0.417	0.002 37	0.230

$$t_{max}=\frac{(E+0.511)^2\beta^4}{\chi_{cc}^2 \ln[b_c(E+0.511)^2\beta^2/\chi_{cc}^2]} \text{ [cm]}, \tag{6}$$

where E is the electron kinetic energy in MeV and b_c and χ_{cc} are constants that depend only on the medium in which the transport takes place. For elements

$$b_c=6702.33\rho \frac{Z^{1/3}(Z+1)}{A} \frac{1}{1+0.000178Z^2} \text{ [cm}^{-1}\text{]}, \tag{7}$$

$$\chi_{cc}=0.39612\sqrt{\frac{Z(Z+1)\rho}{A}} \text{ [MeV cm}^{-1/2}\text{]}, \tag{8}$$

and

$$\chi_c=\chi_{cc}\frac{\sqrt{s}}{(E+0.511)\beta^2} \tag{9}$$

where ρ is the density in g/cm^3, s is the step length in cm, and A is the atomic mass in amu. For polyatomic substances, similar expressions for b_c and χ_{cc} are given by Nelson *et al.*[15] As suggested by Bethe,[13] in Eqs. (7) and (8), $Z^{1/3}(Z+1)$ and $Z(Z+1)$ have been used instead of $Z^{4/3}$ and Z^2, respectively, to take account of inelastic scattering from atomic electrons.

The parameter t_{min} also provides the lower limit on slab thickness (s_{min}) for the present calculations. Values of s_{min} calculated from Eq. (5) with $\Omega_0=20$ for water, air, lead, graphite, and copper in the energy range of 0.5–100 MeV, along with other data, are tabulated in Table I. The value of t_{max} for water, calculated by Bielajew and Rogers,[14] is slightly lower than the CSDA range when $E<3$ MeV, while it is bigger than the CSDA range when $E>3$ MeV.

An important feature of Molière theory is the determination of a more accurate expression for the screening angle (θ_{min}), given by

$$\theta_{min}=\frac{1.13\alpha Z^{1/3}}{\beta(\tau+1)}\sqrt{1.13+3.76\left(\frac{Z}{137\beta}\right)^2}$$
$$=\theta_{min}^{ICRU}\sqrt{1.13+3.76\left(\frac{Z}{137\beta}\right)^2}. \tag{10}$$

The electron mass scattering power can be calculated from Molière theory by

$$\frac{T}{\rho}=\frac{\int_0^{\pi/2} f(\theta)\theta^2 2\pi \sin\theta\, d\theta}{\rho s\int_0^{\pi/2} f(\theta)2\pi \sin\theta\, d\theta}. \tag{11}$$

Calculations with Eq. (11) have been done for various monoenergetic electron beams traversing slabs with thickness in the range (t_{min}, t_{max}). The analytically calculated values of T/ρ are compared with those obtained by the Monte Carlo calculations and are discussed in Sec. IV C. Note that for the analytical calculations: (i) small-angle deflections are not assumed ($d\Omega=2\pi \sin\theta\, d\theta$, not $2\pi\theta\, d\theta$), unlike in ICRU Report 35; (ii) Moller scattering is taken into account; (iii) energy losses are not taken into account (either from bremsstrahlung or secondary-electron production), and (vi) the values of T/ρ are independent of slab thickness provided that the thickness is in the valid range.

III. MONTE CARLO CALCULATIONS

A. EGS4 and user-code MSTEST

The EGS4 (Electron Gamma Shower) Monte Carlo code has been used.[15–17] EGS4 uses the Molière multiple-scattering theory to treat the electron elastic collisions with the atomic nuclei. The EGS4 user-code MSTEST was used to simulate monoenergetic, normally incident pencil beams of electrons passing through slabs of material. MSTEST scores $\overline{\theta^2}$ directly under a variety of conditions discussed below. In particular, one may turn off all Molière multiple

scattering in the code. In most cases $\overline{\theta^2}$ is calculated just for the primary electrons, i.e., excluding the low-energy knock-on electrons.

Initial calculations of the angular distributions calculated by the Monte Carlo technique for very-high-energy electrons (~100 MeV) traversing very thin slabs (with Ω_0 just above 20) were found to be incorrect because the default EGS4 code did not handle the sines and cosines of very small angles correctly (a table look up technique is used for speed). The problem will be discussed in detail elsewhere and this error is corrected in the present calculations.

B. Selection of transport parameters and effect of electron–electron multiple scattering

Some of the electron transport parameters must be chosen with care.[18] In EGS4, the lowest energy at which secondary electrons can be created is defined by the parameter AE (which includes the electron rest mass). Calculations show that AE has an effect on the angular distribution for low-Z materials. This is because the electrons are deflected when they create secondary electrons via Moller interactions and the amount of deflection depends on the production threshold AE.

However, the EGS4 system also accounts for these deflections from the Moller interactions by adjusting the Molière multiple-scattering cross sections as mentioned above regarding Eqs. (7) and (8). In the EGS4 data preparation package, PEGS4, Z^2 is replaced by $Z(Z+\$FUDGEMS)$ with a default value of $\$FUDGEMS=1$. There are bigger differences between Z^2 and $Z(Z+1)$ for low-Z materials than for high-Z materials and thus Moller scatter is relatively more important for low-Z materials.

Thus EGS4 inherently double counts the effects of Moller scatter events which create knock-on electrons above AE. We investigate this double counting of Moller scatter and the AE dependence of $\overline{\theta^2}$ as follows. First, $\overline{\theta^2}_{\text{noms}}$ is calculated with all Molière multiple scattering turned off in the EGS4 simulation. This gives a direct calculation of the deflections modeled by the explicit inclusion of Moller interactions. Figure 1 shows $\overline{\theta^2}_{\text{noms}}$ is strongly AE dependent and the creation of very-low-energy secondaries clearly has a significant effect. Secondly, the size of the Moller scatter contribution to $\overline{\theta^2}$, which is included by using $Z(Z+1)$ instead of Z^2 when creating the PEGS4 data set, is estimated as $\overline{\theta^2} - \overline{\theta^2}_{\text{nomoll}}$, where $\overline{\theta^2}$ is obtained by using the standard EGS4/PEGS4, and $\overline{\theta^2}_{\text{nomoll}}$ is calculated with a PEGS4 data set created with $\$FUDGEMS=0$ (i.e., with no Moller scattering included in the multiple scattering data). Figure 1 shows that $\overline{\theta^2} - \overline{\theta^2}_{\text{nomoll}}$ is almost independent of AE, and is just somewhat greater than $\overline{\theta^2}_{\text{noms}}$ (the estimate based on the explicit modeling of each Moller interaction) if the creation of all secondary electrons down to nearly zero kinetic energy is included. This suggests that both evaluations of Moller scatter are close to equivalent in the limit of considering the creation of all secondary electrons, although the direct calculation eventually fails because it does not account for binding effects. This comparison verifies that using $Z(Z+1)$ instead of Z^2 to account for Moller scatter is a reasonable approximation although Berger and Wang[19] describe a more sophisticated approach.

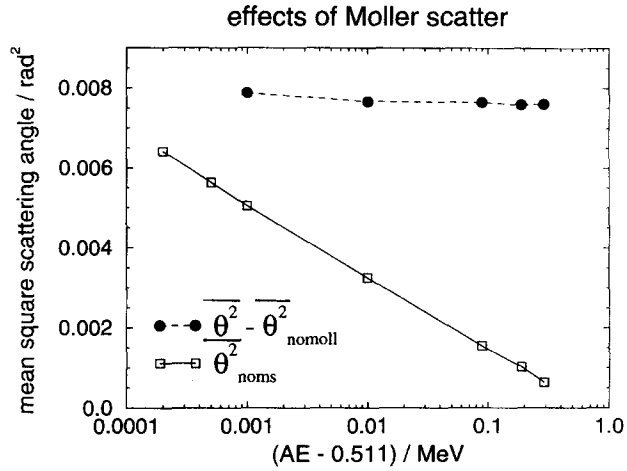

FIG. 1. Mean-square scattering angle caused only by Moller interactions, calculated as a function of (AE-0.511), the kinetic energy threshold for secondary-electron production. Calculations are for 1-MeV electrons traversing a 0.01-cm graphite slab. The contributions from nuclear multiple scattering are excluded. The values of $\overline{\theta^2} - \overline{\theta^2}_{\text{nomoll}}$ include Moller scatter via a $Z(Z+1)$ factor in the PEGS4 data only and values of $\overline{\theta^2}_{\text{noms}}$ include Moller scatter via the simulation in EGS4 of discrete interactions with electrons. Only primary electrons are scored in this calculation.

Thus, an effective mean-square angle of scattering, $\overline{\theta^2}_{\text{eff}}$, which is independent of AE and has the Moller-scatter effect properly accounted for, is

$$\overline{\theta^2}_{\text{eff}} = \overline{\theta^2} - \overline{\theta^2}_{\text{noms}} \ [\text{rad}^2]. \tag{12}$$

The quantity $\overline{\theta^2}_{\text{eff}}$ includes both the contributions from nuclear multiple scattering and Moller scatter accounted for using $Z(Z+1)$ instead of Z^2 in the multiple-scattering formalism. The $\overline{\theta^2}_{\text{noms}}$ term is subtracted so that the Moller scatter from discrete interactions is not double counted. The fractional contribution of Moller scatter to $\overline{\theta^2}_{\text{eff}}$ can be estimated by $(\overline{\theta^2} - \overline{\theta^2}_{\text{nomoll}})/\overline{\theta^2}_{\text{eff}}$, which, as expected, is found to be equal to $[Z(Z+1)-Z^2]/Z(Z+1)[=1/(Z+1)]$ to within 0.1% in a wide variety of situations. Plots of $\overline{\theta^2}$, $\overline{\theta^2}_{\text{eff}}$, and $\overline{\theta^2}_{\text{nomoll}}$ vs AE, calculated for 1-MeV electrons traversing a 0.01-cm graphite slab, are presented in Fig. 2. Table II summarizes the notation used.

A possible alternative to the above approach is to use $\overline{\theta^2}_{\text{nomoll}}$ with a very low value of AE to include the effect of the Moller scatter by simulating it explicitly. However this takes a very long time whereas the $\overline{\theta^2}_{\text{eff}}$ calculations can be done much more quickly with reasonable values of AE.

In contrast to the above, the calculated angular distribution for high-Z materials is not sensitive to AE. For example, for the calculation of 15-MeV electrons traversing a 0.001-cm thick lead slab, 0.80% of the $\overline{\theta^2}$ value is contributed by the Moller scatter when AE=0.900 MeV, compared with 0.86% when AE=521 keV. For high-Z materials, $\overline{\theta^2}_{\text{eff}}$ was found not to differ significantly from $\overline{\theta^2}$.

In general, ESTEPE (the upper limit on the fraction of the energy of an electron lost per step) and ECUT (the minimum

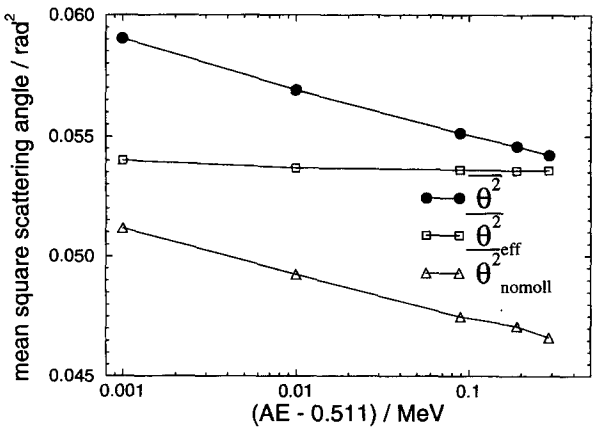

FIG. 2. Dependence on the threshold for the production of secondary electrons, AE, of $\overline{\theta^2}$, $\overline{\theta^2}_{\text{nomoll}}$, and $\overline{\theta^2}_{\text{eff}}=\overline{\theta^2}-\overline{\theta^2}_{\text{noms}}$, calculated for 1-MeV electrons traversing a 0.01-cm graphite slab. The quantity $\overline{\theta^2}$ includes Moller scatter via the $Z(Z+1)$ factor in PEGS4 and via the discrete interactions with electrons simulated in EGS4. $\overline{\theta^2}_{\text{nomoll}}$ includes Moller scatter via electron-discrete interactions in EGS4 only, while $\overline{\theta^2}_{\text{eff}}$ includes Moller scatter via the $Z(Z+1)$ factor in PEGS4 data only. The contributions from nuclear multiple scattering are also included. Only primary electrons are scored in this calculation.

energy for electron transport) have only very small effects on the angular distribution. In the present calculations, ESTEPE has been chosen to be equal to 1% for graphite, air, and water, 0.3% for lead and copper. This ensures that the values of the electron-step size are in the range of $t_{\min}-t_{\max}$. For incident energies less than 1 MeV, ECUT=521 keV and for higher incident energies, 700 keV. For simplicity, we have chosen AE=ECUT for all the materials used in the present calculations. For low-energy runs, especially with high-Z materials, there can be considerable dependence on the values selected for various parameters. In the case of lead this made it impossible to establish (T/ρ) values within 1% below 2 MeV and hence no values are reported.

The remaining transport control parameters are PCUT and AP, the photon equivalents of ECUT and AE. We have chosen 10 keV for these parameters for all the calculations. This properly includes the electron energy loss from the bremsstrahlung effects.

C. Calculation of mass scattering power

It has been found experimentally[20,21] that the increase in the mean-square scattering angle is proportional to slab thickness, s, provided that the mean-square scattering angle is ≤ 0.3 rad^2 (see Sec. IV A). In this region of linearity, we calculate

$$\frac{T}{\rho}=\frac{\overline{\theta^2_{\text{eff}}}}{\rho s} f_E \ [\text{rad}^2\,\text{cm}^2\,\text{g}^{-1}] \tag{13}$$

for an electron-pencil beam traversing a slab, where T/ρ applies to the energy of the electrons *incident* on the slab and f_E is an energy-loss-correction factor which takes into account that the scatter at the back of the slab is from electrons at a range of energies in the slab. As shown below, Eq. (13) gives T/ρ values which are independent of slab thickness (for a range of thicknesses) and thus this equation is equivalent to the differential form given in Eq. (1). For the thin slabs considered here, the energy-loss correction has a small effect on the mass scattering power. Thus it is only necessary to consider the first-order approximation of this correction, which is[22,23]

$$f_E=1-\frac{(S/\rho)_{\text{tot}}\rho s}{E+0.511}, \tag{14}$$

where $(S/\rho)_{\text{tot}}$ is the total mass stopping power and the derivation assumes T/ρ goes as E^{-2}. The correction does not account for energy-loss straggling. In order to keep the uncertainty in the energy-loss correction less than 0.5%, the slab thickness for which $f_E=98\%$ was set to be the maximum thickness $(s_{\max})$ allowed in the calculation. The values of $s_{\max}$ for graphite, water, air, lead, and copper, along with the values of $s_{\min}$, are listed in Table I. Note $s_{\max}$ is much less than $t_{\max}$, the maximum thickness for which the multiple-scattering theory holds.

The code MSTEST tracked up to 40 million electron histories in each case to obtain a statistical precision on $\overline{\theta^2_{\text{eff}}}$ at least as good as 0.5%.

IV. RESULTS

A. Thickness-variation effect

Monte Carlo calculations were done for different slab thicknesses, s, to find the thickness range in which the mass scattering power is well defined and/or can be accurately calculated. The calculated values of $\overline{\theta^2_{\text{eff}}}$ for a 15-MeV electron beam traversing various lead and water slabs are plotted against the slab thickness in Fig. 3. It is seen from Fig. 3 that the increase in $\overline{\theta^2_{\text{eff}}}$ is proportional to s, when $\overline{\theta^2_{\text{eff}}}$ is less than ~ 0.3 rad^2 (region of linearity). For thick slabs there is a satu-

TABLE II. The meanings of the symbols used in Sec. III B as well as in Figs. 1 and 2.

Symbol	Molière multiple scattering from nucleus (Z^2 term)	Moller deflections included in PEGS4 [$Z(Z+1)$ term]	Moller deflections explicitly included in EGS4 (δ rays)
$\overline{\theta^2}$	Yes	Yes	Yes
$\overline{\theta^2_{\text{noms}}}$	No	No	Yes
$\overline{\theta^2_{\text{nomoll}}}$	Yes	No	Yes
$\overline{\theta^2}-\overline{\theta^2_{\text{nomoll}}}$	No	Yes	No
$\overline{\theta^2_{\text{eff}}}=\overline{\theta^2}-\overline{\theta^2_{\text{noms}}}$	Yes	Yes	No

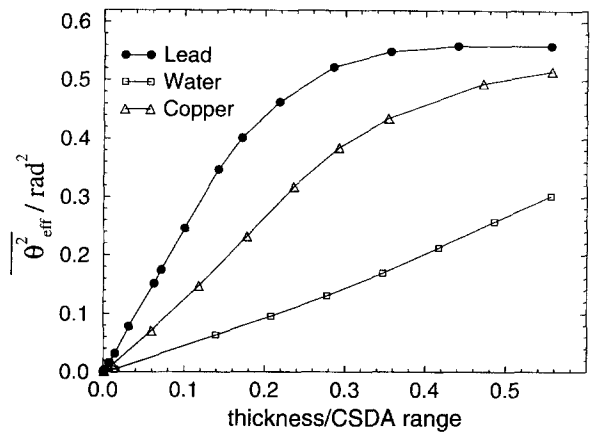

FIG. 3. The values of the mean-square scattering angle $\overline{\theta^2_{\text{eff}}}$, calculated for a 15-MeV electron beam traversing various lead, copper, and water slabs, plotted as a function of the slab thickness. The slab thickness is expressed as a fraction of the CSDA range, which is equal to 7.954, 8.472, and 7.219 g/cm^2 for lead, copper, and water, respectively, at 15 MeV. Only primary electrons are scored in these calculations.

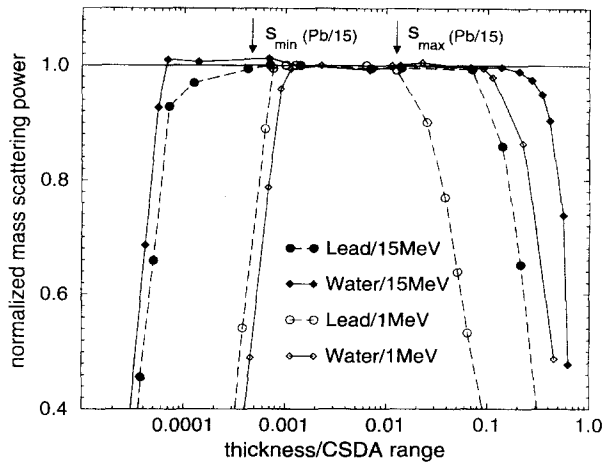

FIG. 4. The Monte Carlo calculated mass scattering powers for 15- and 1-MeV electrons traversing lead and water slabs as a function of slab thicknesses in terms of the CSDA range of the electrons. The CSDA ranges are 7.954 and 7.219 g/cm^2 at 15 MeV and 0.7843 and 0.4367 g/cm^2 at 1 MeV for lead and water, respectively. The T/ρ values are normalized so that the thickness-independent values are equal to 1.

ration of $\overline{\theta^2_{\text{eff}}}$, slightly above ~0.55 rad^2 for lead and ~0.5 rad^2 for copper. For water, $\overline{\theta^2_{\text{eff}}}$ saturates when the slab thickness is greater than ~70% of the CSDA range. This saturation is because electrons scattered at large angles do not get out of the slab. Figure 3 shows that the region of linearity becomes wide if the atomic number is low. It should be noted that the proportionality shown in Fig. 3 is not entirely due to the mass scattering power at the initial energy because the energy loss of electrons and the consequent gradual increase in scattering power has to be taken into account in thick slabs.

The mass scattering powers as calculated by Eq. (13) for 15- and 1-MeV electrons traversing lead and water slabs are plotted in Fig. 4 as functions of the slab thickness. The T/ρ values are normalized so that the thickness-independent values are equal to 1. The plot shows that the calculated mass scattering power is independent of the thickness in the range of 0.001–0.5 g/cm^2 (flat region) for 15-MeV electrons or 0.001–0.1 g/cm^2 for 1-MeV electrons. This figure shows that the electron mass scattering power is a well behaved quantity in the flat region of slab thickness in the sense that the average square of the scattering angle increases at a constant rate, independent of the value of $\overline{\theta^2}$ which is constantly increasing as the slab thickness increases. This justifies using $\overline{\theta^2}$ in Eq. (13) instead of $d\overline{\theta^2}$ as in Eq. (1). For slab thicknesses which are greater than those of the flat region, the decrease of the mass scattering power is due to the saturation of $\overline{\theta^2_{\text{eff}}}$ observed in Fig. 3 and due to the large energy-loss effect which is no longer properly accounted for by f_E. For slabs this thick, the concept of mass scattering power is no longer valid. When the slab thickness is too thin, the breakdown of the multiple-scattering theory results in the underestimation of the mass scattering power. This represents a breakdown in the Monte Carlo calculation although the concept of the mass scattering power continues to apply for thin slabs.

In the following calculations of T/ρ, we have chosen the slab thickness within the range of $s_{\min}-s_{\max}$ (Table I), which is in the flat region. It should be noted here that the contribution from secondary electrons is excluded from $\overline{\theta^2_{\text{eff}}}$ since T/ρ refers to only primary electrons. A calculation for 1-MeV electrons traversing a 0.007-cm thick graphite slab shows that if included in the calculation, secondary electrons would make a 0.3% contribution to $\overline{\theta^2_{\text{eff}}}$. The effect of secondary electrons is much greater for thicker slabs. (For more details about secondary-electron effect, see Sec. IV C.) However, for the thin slabs considered in the calculations of T/ρ, the effect of secondary electrons would not be significant.

B. T/ρ versus energy

Electron mass scattering powers were calculated in the energy range of 0.5–100 MeV, which encompasses the range of energies of interest in radiotherapy. Three arbitrary thicknesses were chosen from the range of $s_{\min}-s_{\max}$ to calculate the T/ρ value for each energy. The mean of the three mass scattering powers are tabulated in Table III for water, air, graphite, copper, and lead.

It is found that, for high-Z material (lead), the T/ρ values for low ($E \leq 2$ MeV) and high energies ($E \geq 20$ MeV) vary somewhat with the slab thickness. For low energies this variation may reflect problems with the simulation since multiple scattering is substantial. For this reason, and because of the sensitivity to parameters discussed in Sec. III B, we do not present data for lead below 2 MeV and for all materials the uncertainty may go up to ±1% for values with energies below 1 MeV. At high energies, bremsstrahlung becomes significant. Although the electron angular deflection caused by bremsstrahlung events is not included in EGS4, the occasional energy loss caused by the bremsstrahlung events causes the mass scattering power to increase because the lower-energy (but still primary) electrons scatter more. It is found that the T/ρ value for 100-MeV electrons on lead increases by 20% as Ω_0 increases from 100 to 1000 (by 9%

TABLE III. Monte Carlo calculated electron mass scattering powers (rad^2 cm^2 g^{-1}, values have been multiplied by 100). The one standard deviation statistical uncertainty on the Monte Carlo T/ρ is generally ±0.5%. The overall uncertainty on T/ρ is ±2%. The data marked by "*" exhibit a variation with slab thickness and are the mean of T/ρ values calculated for Ω_0 between 100 and 200. The lead values marked by "#" are too sensitive to the transport parameters to allow accurate values to be determined.

Kinetic energy (MeV)	Water ×100	Air ×100	Graphite ×100	Copper ×100	Lead ×100
0.5	1065	1052	884	3030	#
0.8	517	511	436	1506	#
1	368	365	310	1081	#
2	126.0	124.2	107	372	#
3	65.9	65.2	55.3	195.5	411
4	40.4	40.4	34.1	122.2	259
5	27.7	27.7	23.5	83.7	178.9
6	20.32	20.32	17.22	61.6	131.7
8	12.39	12.44	10.49	37.4	80.6
10	8.40	8.29	7.02	25.4	54.8
15	4.01	4.01	3.40	12.36	26.9
20	2.43	2.397	2.032	7.35	16.13*
30	1.155	1.141	0.960	3.55	7.79*
40	0.683	0.674	0.570	2.075	4.63*
50	0.452	0.446	0.377	1.374*	3.07*
60	0.323	0.319	0.270	0.987*	2.216*
80	0.1905	0.1882	0.1579	0.577*	1.312*
100	0.1258	0.1245	0.1048	0.383*	0.874*

for copper). The T/ρ values tabulated in Table III for lead and copper for high energies, which are marked by "*," are the average of T/ρ values calculated for $100 \leq \Omega_0 \leq 200$. Even these values contain a significant contribution from bremsstrahlung events (e.g., 3% of 100-MeV electrons passing through a lead slab with $\Omega_0 = 100$ lose energy creating a bremsstrahlung photon). For low-Z materials, even at 100 MeV, the variation with slab thickness is much less (≤2%).

A plot of the mass scattering power versus electron kinetic energy (E) for lead and graphite is shown in Fig. 5. For comparison, the values of T/ρ tabulated in ICRU Report 35 are also included. The relationship on a log–log scale shows a steady and almost linear drop of T/ρ with an increase in electron energy, suggesting a relatively simple relation, $T/\rho \propto E^{-n}$, where n is in the range of 1.5–2.0 depending on E. In particular, $n = 1.5$ when $E \sim 1$ MeV for both high-Z (lead) and low-Z (graphite) materials, while, when $E \sim 60$ MeV, $n = 2.0$ or 1.85 for high-Z or low-Z materials, respectively. This is comparable to the fit to the data of ICRU Report 21 done by Werner *et al.* where n was found to be equal to 1.78 for materials from water to aluminum in an energy range of 5–20 MeV.[24]

Figure 6 presents the percentage difference between the Monte Carlo calculated values of T/ρ and those in ICRU Report 35 which did not include the contribution from Moller scatter in the tabulated T/ρ values. As recommended by ICRU Report 35 and as verified above, multiplication by $Z(Z+1)/Z^2$ is an approximate way to modify the ICRU 35 values to include the Moller scatter contribution. Figure 7 presents the percentage difference between the Monte Carlo and the modified ICRU 35 values.

The differences between the Monte Carlo and ICRU 35 results exhibit a very limited energy dependence for energies between 1 and 25 MeV for high-Z materials and for energies less than 60 MeV for low-Z materials. The differences increase as electron energy increases above these values and is as much as 30% when $E = 100$ MeV for both cases. One of the reasons is that Eq. (2) used for calculating ICRU35 values is only valid for intermediate energies since the effects of the finite size of the nucleus and electron screening were not considered rigorously when Eq. (2) was derived.[3] These effects limit the validity of the results to a certain range of energies, viz., those for which $\beta\tau < 280A^{-1/3}$.[23] The upper limits on electron energy for using Eq. (2) are approximately 24 and 62 MeV for lead and graphite, respectively. The

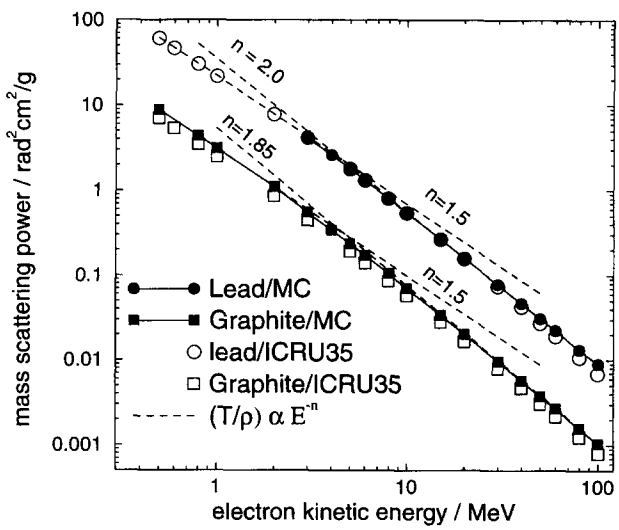

FIG. 5. Electron-energy dependence of the mass scattering power for lead and graphite in the energy range of 0.5–100 MeV. Monte Carlo and ICRU Report 35 values are included for comparison. The relation $T/\rho \propto E^{-n}$, where n is in the range of 1.5–2.0 depending on E, fits the Monte Carlo calculations.

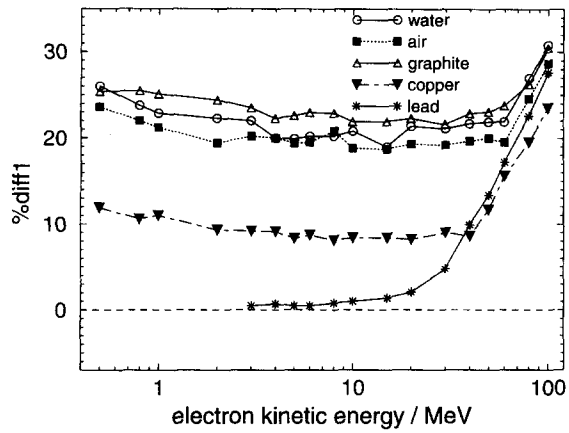

FIG. 6. Percentage difference between the present Monte Carlo results and those of ICRU Report 35 where %diff1 = 100[(MC − ICRU35)/ICRU35], with MC and ICRU35 representing T/ρ values from the present Monte Carlo calculation and from ICRU Report 35, respectively.

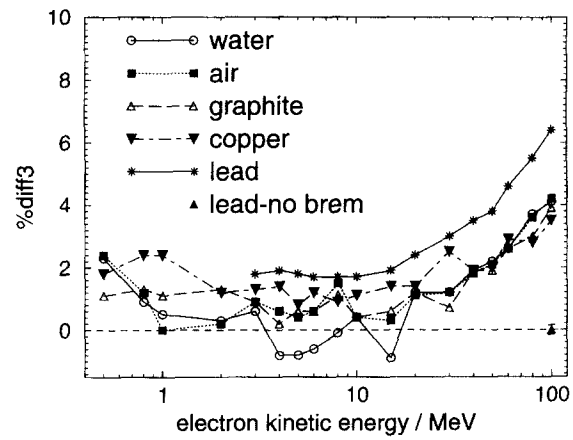

FIG. 8. Percentage difference between the Monte Carlo results and the analytical values where %diff3 = 100[(MC − analytic)/MC]. The value at 100 MeV labeled as "lead-no brem" is calculated for a lead slab with $\Omega_0 = 1000$ and with no bremsstrahlung production simulated.

worsening agreement with the present Monte Carlo calculation shown in Figs. 6 and 7 is consistent with these limits. Another reason for the disagreement is the bremsstrahlung effect at higher energies as discussed above.

For energies below ~60 MeV, the Monte Carlo values for low-Z materials are approximately 22% higher than those in ICRU Report 35, while there is only about a 1% difference between 1 and 25 MeV for the high-Z material (lead). This is mainly because the effect of electron–electron multiple scattering on T/ρ values is more significant for low-Z materials than that for high-Z material and Moller scatter is not included in the ICRU35 values.

At energies less than 60 MeV, for low-Z materials as well as copper the Monte Carlo values are approximately 6% higher than the ICRU Report 35 values modified for Moller scatter. Note that this difference is in the opposite direction from the results of McParland.[7]

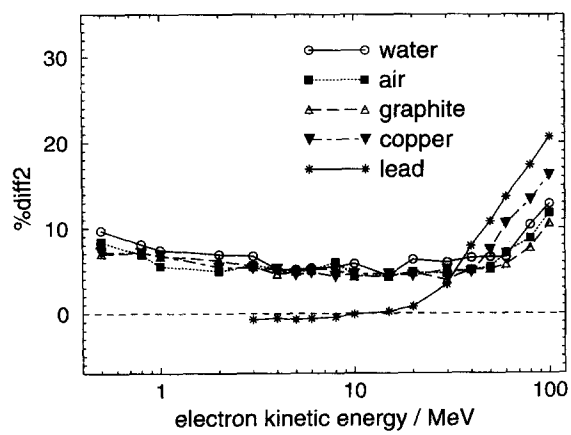

FIG. 7. Percentage difference between the present Monte Carlo results and the modified ICRU 35 values where %diff2 = 100{MC − ICRU35[$Z(Z+1)/Z^2$]/MC}.

C. Comparison to analytic calculations

Figure 8 presents the percentage difference versus energy between the values of T/ρ calculated by the Monte Carlo method compared with those calculated analytically by Eq. (11). The Monte Carlo values agree with the analytical values within 2% up to 20 MeV for high-Z materials and to 50 MeV for low-Z materials while the difference increases when electron energy is beyond these values. For very high energy, the higher difference is caused by bremsstrahlung events which cause some of the primary electrons to have much lower energies and thus scatter more. To demonstrate this, a run was done without simulating bremsstrahlung discrete events (AP = 100 MeV) for 100-MeV electrons on a lead target with $\Omega = 1000$. In this case the Monte Carlo calculations agree with the analytic values within the 0.15% precision of the calculations.

There remains a residual 1% to 2% discrepancy at lower energies. This may result from slightly different numerical methods used to evaluate the Moliere distribution in the analytic and Monte Carlo calculations.

The Monte Carlo values of T/ρ are based on the same multiple-scattering theory as the analytic calculations but the Monte Carlo values are more realistic. The Monte Carlo method has taken into account the effects of large energy-loss events (i.e., energy-loss straggling) from the creation of knock-ons and bremsstrahlung. Thus, in general, the data calculated by the Monte Carlo method are recommended although in the energy range of interest to radiotherapy there is no practical difference.

D. Comparison to experiment and discussion of uncertainties

Comparison to experimental data is the ultimate test of any calculation. However, precise experimental data for electron mass scattering powers are lacking. An experiment that is considered by many to be a benchmark for testing electron multiple scattering at low energies (15.7-MeV electrons on gold) was reported by Hanson *et al.*[11] Their results agree

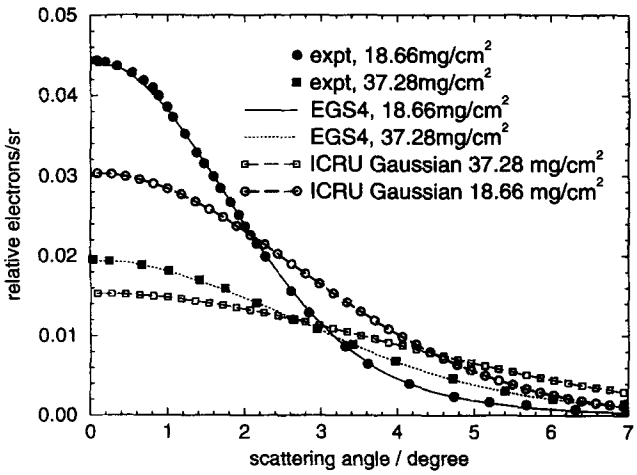

FIG. 9. Comparison of the angular distributions calculated by the present EGS4 Monte Carlo technique with those measured by Hanson *et al.* (Ref. 11) and those calculated using a Gaussian distribution with the ICRU Report 35's value of T/ρ, for 15.7 monoenergetic electrons traversing 18.66 and 37.28 mg/cm^2 thick gold slabs.

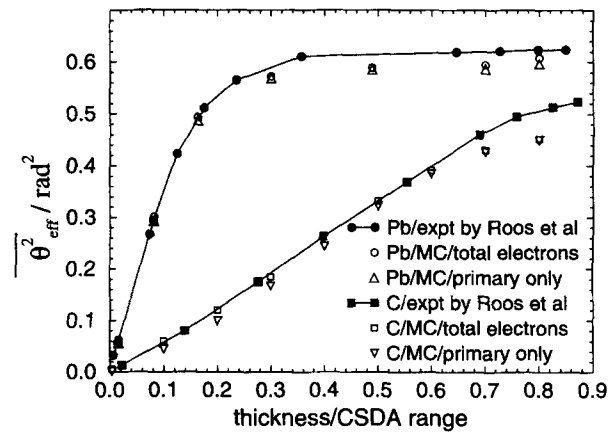

FIG. 10. Comparison of the $\overline{\theta^2_{\text{eff}}}$ values calculated for 10-MeV electrons traversing various lead and graphite slabs with the experimental data reported by Roos *et al.* (Ref. 20). Note that the experimental data include the effects of the primary and the secondary electrons, which are found to be in good agreement with present $\overline{\theta^2_{\text{eff}}}$ values calculated for the primary and the secondary electrons, except for very thick slabs. The $\overline{\theta^2_{\text{eff}}}$ values calculated for only the primary electrons are also plotted to show the scattering contribution from the secondary electrons. The electron CSDA range is equal to 6.133 and 5.657 g/cm^2 for lead and graphite, respectively, at 10 MeV.

with EGS3 calculations[16] and with the present EGS4 calculation as seen from Fig. 9. The Gaussian angular distributions calculated using the ICRU Report 35 value for $\overline{\theta^2}$ are also shown in Fig. 9. As recognized by ICRU Report 35, this Gaussian disagrees with the experimental data and with the EGS4 Monte Carlo results. The central peak in the experimental data for the thinner target can be fit by a much narrower Gaussian distribution ($\overline{\theta^2} = 1.97 \times 10^{-3}$ rad^2 compared to $\overline{\theta^2} = 4.46 \times 10^{-3}$ rad^2 for both the Molière and ICRU calculations). In ICRU Report 35 it is shown that the Gaussian term of the Molière theory (used in Ref. 8 to calculate T/ρ) also fails to fit the central Gaussian shape very well.

One must be careful interpreting Fig. 9. It demonstrates that both the Molière theory and the EGS4 code predict the angular distribution well and thus we can conclude the calculated T/ρ is correct. The disagreement of the Gaussian curve demonstrates the failure of the Gaussian model and not the inaccuracy of the value of T/ρ, which is given correctly in this case by Rossi's theory.

Roos *et al.*[20] have presented data on the mean-square scattering angle measured for various targets and electron energies. Their data include primary and secondary electrons. For comparison, the contribution of secondaries to the mean-square scattering angle has been taken into account in our calculations of 10-MeV electrons traversing various lead and graphite slabs. In the calculation of $\overline{\theta^2_{\text{eff}}}$, the fraction of Moller scatter when both primary and secondary electrons were scored was assumed to be equal to that when only the primary electrons were scored. The present Monte Carlo results, along with the experimental measurements of Roos *et al.*, are plotted in Fig. 10. Except for very thick slabs, the experimental data are in good agreement with our $\overline{\theta^2_{\text{eff}}}$ values calculated for primary and secondary electrons (within $\pm 1.5\%$ for $\overline{\theta^2_{\text{eff}}} < 0.3$ rad^2 for graphite and < 0.5 rad^2 for lead). These data suggest a preference for the Monte Carlo values of T/ρ compared to the ICRU values. The $\overline{\theta^2_{\text{eff}}}$ values calculated for only primary electrons are also plotted in Fig. 10 in order to show the effects from the secondary electrons.

Recently, Blais and Podgorsak[25] have indirectly measured T/ρ in air for several energies. It is difficult to make a direct comparison of their T/ρ data with ours because the energies corresponding to the T/ρ values are also deduced from the T/ρ data by using the ICRU values of T/ρ vs E. (Note that the T/ρ data they used to derive the corresponding energies are those of ICRU Report 35 modified to include Moller scatter.) However, by combining their data with the results obtained by other energy-determination methods mentioned in their article, an indirect comparison has been made which shows that the present calculated T/ρ data agree with their measurements within ~4% but the accuracy is not adequate to discriminate between the various calculations of T/ρ.

A measurement of electron multiple scattering in air for 5.9-MeV electrons was reported by Brahme.[26] The T/ρ value, calculated from the measured angular distribution in his article is found to be ~15% lower than the present Monte Carlo value and ~10% lower than that in ICRU Report 35 if the effects of Moller scatter are taken into account. The width of his experimental angular distribution is 12% wider than we calculate. This suggests that a larger T/ρ value should be extracted from the experimental data and yet a smaller value was determined.

Monte Carlo calculations have been shown to provide accurate simulation of electron transport, as long as the actual geometry is modeled closely enough.[17,27] High accuracy is expected for the present calculation since the actual geometry can be modeled almost exactly. The uncertainties in the present calculation come from statistical and systematic considerations. The statistical uncertainty was below 0.5% (1 standard deviation). The uncertainties in $\overline{\theta^2_{\text{eff}}}$ and f_E in Eq. (13) dominate systematic uncertainties. Since the energy loss

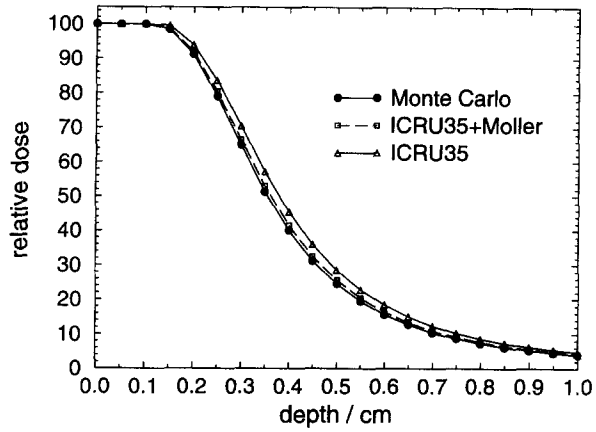

FIG. 11. Depth-dose distributions for a 5-MeV electron beam with 0.1 cm ×0.1 cm field size at the surface of the water, calculated by using the Hogstrom pencil-beam code with T/ρ values from the present Monte Carlo calculations, from ICRU Report 35 and from ICRU Report 35 but modified to include Moller scatter. The depth-dose data measured for 10 cm×10 cm field size are input in this calculation. In terms of agreement, this is a worst case due to the extremely small field size.

is limited to 2% by our choice of s_{max} and the energy-loss correction given by Eq. (14) is accurate for thin slab thickness, f_E is treated as having 0.5% uncertainty. The uncertainty of $\overline{\theta^2_{eff}}$ is governed mainly by the choices of the Monte Carlo transport parameters as described in Sec. II C and the overall uncertainty in the Monte Carlo technique. In view of the good agreement with the high-quality data of Hanson *et al.* and Roos *et al.*, a reasonable estimate of the overall uncertainty on the Monte Carlo T/ρ data is ±2% (1 standard deviation).

E. Impact on electron-beam treatment planning

The mass scattering power is used in most pencil-beam treatment planning algorithms.[5,28] We have investigated the influence of different T/ρ values on the dose in a homogeneous water phantom calculated using the well-known Hogstrom pencil-beam code.[28] We used the Monte Carlo T/ρ values and those of ICRU Report 35, both with and without the effects of electron–electron multiple scattering. The Hogstrom algorithm forces a fit to the central-axis depth-dose curve in a 10 cm×10 cm incident beam and thus the central-axis depth-dose curve in a broad beam is independent of T/ρ values. However the T/ρ values do affect the shape of individual pencil beams and thus affect the depth-dose curve for small field size or the penumbra in broad beams. The depth-dose distribution for a 5-MeV electron pencil beam with 0.1 cm×0.1 cm field size at the surface of the water phantom is shown in Fig. 11. It shows about a 10% difference in the depth-dose curves calculated using the present Monte Carlo T/ρ data versus using ICRU35 T/ρ data. This figure shows a worst case situation due to the extremely small field size considered and demonstrates the effects on an elemental pencil beam. Similar calculations were done for several energies of electron beams with various field sizes in a water phantom. As expected no difference was found in the dose distributions between using the three sets of T/ρ values for a 5-MeV electron beam with a broad 5 cm×5 cm field size. For a higher nominal electron-beam energy, 18 MeV, a general difference of about 7% was found in the relative depth-dose distributions between using the three sets of T/ρ values for a 0.1 cm×0.1 cm field size, while a difference of about 3% was observed for a 4 cm×4 cm field size. The use of high quality T/ρ data, which should include the effect of electron–electron multiple scattering, has an effect on elemental pencil beams. This means it will have direct effects in calculations for small beams and in the penumbral region. It also suggests effects are possible in nonhomogeneous phantoms at other points in the beam.

The present study shows that T/ρ is only well behaved up to a given slab thickness. This suggests that in the implementation of pencil-beam codes the depth step should be chosen with care, especially for small field size, in order to avoid problems. The values of s_{max}, tabulated in Table I, are a conservative upper limit on the depth step since for much greater steps one may encounter the region of rapid drop off for large steps seen in Fig. 4. Setting the maximum depth step to be equal to s_{max} ensures that the correction needed for energy loss in each depth step is less than 2%. This may be too conservative and Fig. 4 suggests that steps up to 10% of the residual CSDA range may be acceptable.

V. CONCLUDING REMARKS

The results demonstrate that the concept of mass scattering power is valid since values calculated for different slab thicknesses are the same. Eventually the concept breaks down for very thick slabs. The Monte Carlo values of electron mass scattering power are more accurate than previous values. This is primarily because they are based on the Molière multiple-scattering theory which is more accurate than the simple models used in ICRU Report 35. The Monte Carlo calculated values are generally in good agreement with our analytic calculations based on the Molière theory, except above 20 MeV where effects of bremsstrahlung induced energy-loss straggling cause the Monte Carlo values to increase by up to 20% (for 100-MeV electrons on a lead slab with $\Omega=1000$.). The Monte Carlo and analytic Molière calculations account for the effects of Moller scattering from electrons by replacing Z^2 by $Z(Z+1)$ in the appropriate formulas. Explicit calculations of the effects of Moller scatter show that this is a reasonable approximation although it may be a slight overestimate.

The Monte Carlo values of T/ρ tend to be about 6% larger than the ICRU Report 35 values (adjusted for Moller scatter) for low- and medium-Z materials in the most important energy range for radiotherapy. We have investigated several aspects of this to see which approximations may be breaking down. In the ICRU's expression there are fairly arbitrary and simple models of θ_{min} and θ_{max} which take into account screening and the finite size of the nucleus, respectively. We find that varying θ_{min} in the analytic expressions has a small effect on the values of T/ρ. Using Molière's value of θ_{min} in the ICRU expression makes agreement somewhat worse. The value of θ_{max} is more critical and although an arbitrary cap on θ_{max} of 1 is traditionally used, increasing this value to $\pi/2$ would significantly increase the ICRU's values of T/ρ. We

also investigated one aspect of the use of the small-angle approximation by using the small-angle approximation for the solid angle in Eq. (11) (i.e., using $2\pi\theta\, d\theta$ instead of $2\pi \sin\theta\, d\theta$). This increased the Molière calculated values of T/ρ by 4% or 5%, even for very thin slabs because the tails of the distribution are so important.

However, all of the above considerations are somewhat secondary. Although the values of T/ρ calculated by various ways are close to each other, the actual distributions predicted by the Gaussian models versus the Molière theory are very different. Figure 9 emphasizes the importance of the single scattering tails in the calculation of T/ρ. In this high-Z case the values of T/ρ calculated by the Monte Carlo (Molière) method or the simple analytic models are very similar and yet the Gaussian angular distribution with the corresponding value of $\overline{\theta^2}$ is much too broad. As discussed in ICRU Report 35,[4] the central peak is indeed Gaussian but with a much smaller width. This lack of agreement with the simple Gaussian shape is a well-known flaw and a variety of approaches to overcome it have been tried.[29,30] This lack of agreement with the fundamental Gaussian shape suggests that the use of the improved values of T/ρ calculated here will not significantly improve results deduced using Gaussian models. Perhaps a more useful approach would be to tabulate values corresponding to the central Gaussian peak in the Molière distribution (as opposed to using the just the Gaussian term in the Molière distribution[8]). These are unfortunately a function of slab thickness but there is some indication they could be parameterized.[4] It is not clear whether this would improve the simple models for electron-beam treatment planning but it might be useful for various other applications.

ACKNOWLEDGMENTS

One of the authors (X.L.) is grateful to the Fonds pour la Formation de Chercheurs et l'Aide à la Recherche (Québec) Postdoctoral Fellowship. Our thanks go to Jiansheng Sun, Bruce Faddegon, and George Ding for lively help with the computer systems, and Ruqing Wang and Alex Bielajew for useful discussions on the subject. Special thanks to Alex Bielajew for giving us a function routine for calculating the Molière distribution and to Barry Werner, Anders Brahme, and two anonymous referees for very helpful comments on the manuscript.

[a]Present Address: Ottawa Regional Cancer Centre, Department of Medical Physics, Civic Division, 190 Melrose Avenue, Ottawa, Canada K1Y 4K7.
[b]E-mail: dave@irs.phy.nrc.ca, Tel: (613) 993-2715, Fax: (613) 952-9865.

[1]ICRU, "Radiation Dosimetry: Electrons with Initial Energies Between 1 and 50 Mev," ICRU Report 21 (Bethesda, MD) (1972).
[2]A. Brahme, "On the optimal choice of scattering foils for electron therapy," TRITA-EPP 72-17, Royal Inst. of Technology, Stockholm, Sweden (1972).
[3]B. B. Rossi, *High Energy Particles* (Prentice Hall, New York, 1952).
[4]ICRU, "Radiation Dosimetry: Electron beams with energies between 1 and 50 MeV," ICRU Report 35, Bethesda, MD (1984).
[5]K. R. Hogstrom, M. D. Mills, and P. R. Almond, "Electron beam dose calculations," Phys. Med. Biol. **26**, 445–459 (1981).
[6]A. F. Bielajew, "Plural and multiple small-angle scattering from a screened Rutherford cross section," Nucl. Instrum. Methods B **86**, 257–269 (1994).
[7]B. J. McParland, "A derivation of the electron mass scattering power for electron dose calculations," Nucl. Instrum. Methods A **274**, 592–596 (1989).
[8]H. Huizenga and P. R. M. Storchi, "Numerical calculation of energy deposition by broad high-energy electron beams," Phys. Med. Biol. **34**, 1371–1396 (1989).
[9]G. Z. Molière, "Theorie der Streuung schneller geladener Teilchen. I. Einzelstreuung am abgeschirmten Coulomb-Field," Z. Naturforsch a**2**, 133–145 (1947).
[10]G. Z. Molière, "Theorie der Streuung schneller geladener Teilchen. II. Mehrfach- und Vielfachstreuung," Z. Naturforsch. a**3**, 78–97 (1948).
[11]A. O. Hanson, L. H. Lanzl, E. M. Lyman, and M. B. Scott, "Measurement of multiple scattering of 15.7-MeV electrons," Phys. Rev. **84**, 634–637 (1951).
[12]A. F. Bielajew, R. Wang, and S. Duane, "Incorporation of single scattering in the EGS4 Monte Carlo code system: Tests of Moliere theory," Nucl. Inst. Methods B **82**, 503–512 (1993).
[13]H. A. Bethe, "Molière's theory of multiple scattering," Phys. Rev. **89**, 1256–1266 (1953).
[14]A. F. Bielajew and D. W. O. Rogers, "PRESTA: The parameter reduced electron-step transport algorithm for electron Monte Carlo transport," Nucl. Instrum. Meth. B **18**, 165–181 (1987).
[15]W. R. Nelson, H. Hirayama, and D. W. O. Rogers, "The EGS4 code system," Stanford Linear Accelerator Center Report SLAC-265 (Stanford Calif) (1985).
[16]R. L. Ford and W. R. Nelson, "The EGS code system—Version 3," Stanford Linear Accelerator Center Report SLAC-210 (1978).
[17]W. R. Nelson and D. W. O. Rogers, "Structure and operation of the EGS4 code system," in *Monte Carlo Transport of Electrons and Photons Below 50 MeV*, edited by T. M. Jenkins, W. R. Nelson, A. Rindi, A. E. Nahum, and D. W. O. Rogers (Plenum, New York, 1989), pp. 287–306.
[18]D. W. O. Rogers, "Low-energy electron transport with EGS," Nucl. Instrum. Methods **227**, 535–548 (1984).
[19]M. J. Berger and R. Wang, "Multiple-scattering angular deflections and energy-loss straggling," in *Monte Carlo Transport of Electrons and Photons Below 50 MeV*, edited by T. M. Jenkins, W. R. Nelson, A. Rindi, A. E. Nahum, and D. W. O. Rogers (Plenum, New York, 1989), pp. 21–56.
[20]H. Roos, P. Drepper, and D. Harder, "The transition from multiple scattering to complete diffusion of high energy electrons," Proc. of 4th Symposium on Microdosimetry (Commis. of Eur. Comm. EUR 5122) 779–798 (1973).
[21]H. J. Schulz, "Aufbau des Sekundärelektronenenspektrums energiereicher Elektronen; ein spezielles Problem des Durchgangs von Elektronen durch Materie," Dissertation Würzburg, 1970.
[22]L. Eyges, "Multiple scattering with energy loss," Phys. Rev. **74**, 1534 (1948).
[23]A. Brahme, "Simple relations for the penetration of high-energy electron beams in matter," SSI: 1975-011, Dep. Radiation Physics, Karolinska Institute, Stockholm, Sweden (1975).
[24]B. L. Werner, F. M. Khan and F. C. Deibel, "A model for calculating electron beam scattering in treatment planning," Med. Phys. **9**, 180–187 (1982).
[25]N. Blais and E. B. Podgorsak, "The mass angular scattering power method for determining the kinetic energies of clinical electron beams," Phys. Med. Biol. **37**, 1931–1942 (1992).
[26]A. Brahme, "Multiple scattering of relativistic electrons in air," TRITA-EPP 71-22, Royal Inst. of Technology, Stockholm, Sweden (1971).
[27]D. W. O. Rogers and A. F. Bielajew, "Monte Carlo techniques of electron and photon transport for radiation dosimetry," in *The Dosimetry of Ionizing Radiation*, edited by K. R. Kase, B. E. Bjarngard, and F. H. Attix (Academic, New York, 1990), Vol. III, pp. 427–539.
[28]K. R. Hogstrom, "Evaluation of electron pencil beam dose calculation," Med. Phys. Monograph (AAPM) No. 15, 532–561 (1986).
[29]I. Lax, A. Brahme, and P. Andreo, "Electron-beam dose planning using Gaussian beams," Acta Radiol. **364**, 49–59 (1983).
[30]D. Jette and A. F. Bielajew, "Electron dose calculation using multiple-scattering theory: Second-order multiple-scattering theory," Med. Phys. **16**, 698–711 (1989).